*Pure & Appl. Chem.*, Vol.55, No.1, pp.77-87, 1983.
Printed in Great Britain.

0033-4545/83/010077-11$03.00/0
Pergamon Press Ltd.


# METALLOBORANE CLUSTER COMPOUNDS

Norman N. Greenwood

Department of Inorganic and Structural Chemistry,
University of Leeds, Leeds LS2 9JT, England

Abstract - Recent work has shown that most transition metals and post-transition metals can be incorporated as vertices in polyhedral metalloborane cluster compounds. Numerous synthetic routes have been devised and structural studies on the resulting clusters have revealed an astonishing variety of geometrical forms. Most boranes and borane anions from $B_2$ to $B_{12}$ now have metalloborane analogues in which one or more of the various boron atoms in the cluster of the parent borane are replaced by a metal centre. In addition, the flexibility introduced into the bonding by the differing connectivities, coordination numbers, and oxidation states of the various metals enables many unprecedented clusters to be generated. Examples of these novel cluster geometries include *conjuncto*-$[(PMe_2Ph)_2(Pt_2B_8H_{14})]$, *conjuncto*-$[(PMe_2Ph)_2(Pt_2B_{12}H_{18})]$, *iso-nido*-$[(PPh_3)_2(IrB_9H_{10}.PPh_3)]$, *iso-closo*-$[H(PPh_3)(PPh_2\overline{C_6H_4})(\overline{IrB_9H_8})]$, *iso-closo*-$[H(PMe_3)_2(IrB_8H_7Cl)]$, *conjuncto*-$[(PMe_2Ph)(PtB_{16}H_{18}.PMe_2Ph)]$, and several *conjuncto*-$PtB_{18}$ and -$Pt_2B_{18}$ species some of which feature the construction by cluster rearrangement of an unusual confacial triangular fusion between the two subclusters.

## INTRODUCTION

At the 19th ICCC in Prague four years ago we organized a Microsymposium on the theme of "Boranes as Ligands" and the seven papers presented there gave some idea of how far this novel approach to boron hydride chemistry had developed at that time (ref.1). A wide variety of cluster complexes has now been synthesized in which boranes act as polyhapto ligands to both transition metals and post-transition metals. Coordination can be via B-H→M or $B_n$→M bonds (or both) and all hapticities from $\eta^1$ to $\eta^6$ have been characterized (ref. 2). In those cases where only $B_n$-M interactions are involved in the cluster bonding, it is sometimes helpful to think of the resulting complex not as a coordination compound but as a metalloborane cluster in which the metal centres and the BH groups combine to form the polyhedral cluster. Indeed, most metals (in common with boron) have fewer valency electrons than orbitals available for bonding and so can be considered as honorary boron atoms. Or perhaps one should say flexi-boron atoms because, by appropriate choice of metal and pendant ligands, it is often possible to vary both the number of electrons contributed and the number of orbitals provided by the metal atom(s) to the cluster.

Boron itself always formally contributes 2 electrons and 3 orbitals to cluster bonding in the parent boranes and in related compounds such as the carbaboranes, and this forms the basis for the well known Wade's rules (ref. 3). Several series of boranes and their derivatives are now recognized and their structures can be rationalized according to the number of skeletal electrons available for cluster bonding, as shown in Table 1.

TABLE 1. Borane structures - Wade's rules

| Series | Parent Formula | Skeletal Electrons | Cluster Geometry (deltahedron = closed triangulated polyhedron) |
|---|---|---|---|
| *precloso-* | $B_nH_n$ | 2n | (n-1) vertexed deltahedron plus 1 capping BH |
| *closo-* | $B_nH_{n+2}$ | 2n+2 | n-vertexed deltahedron |
| *nido-* | $B_nH_{n+4}$ | 2n+4 | (n+1) deltahedron (n occupied) |
| *arachno-* | $B_nH_{n+6}$ | 2n+6 | (n+2) deltahedron (n occupied) |
| *hypho-* | $B_nH_{n+8}$ | 2n+8 | (n+3) deltahedron (n occupied) |
| *conjuncto-* | $B_nH_m$ | - | two or more clusters joined by B-B or BBB bonds, or by sharing common vertices, edges, or faces |

So far as metals are concerned, virtually every metal in the periodic table can serve as a vertex in metalloborane cluster compounds providing the electronegativity difference between the metal and boron is not greater than about 0.5 on the Pauling scale. As illustrated in Fig. 1, this includes all metals except the most electropositive ones in Groups IA, IIA, IIIA,

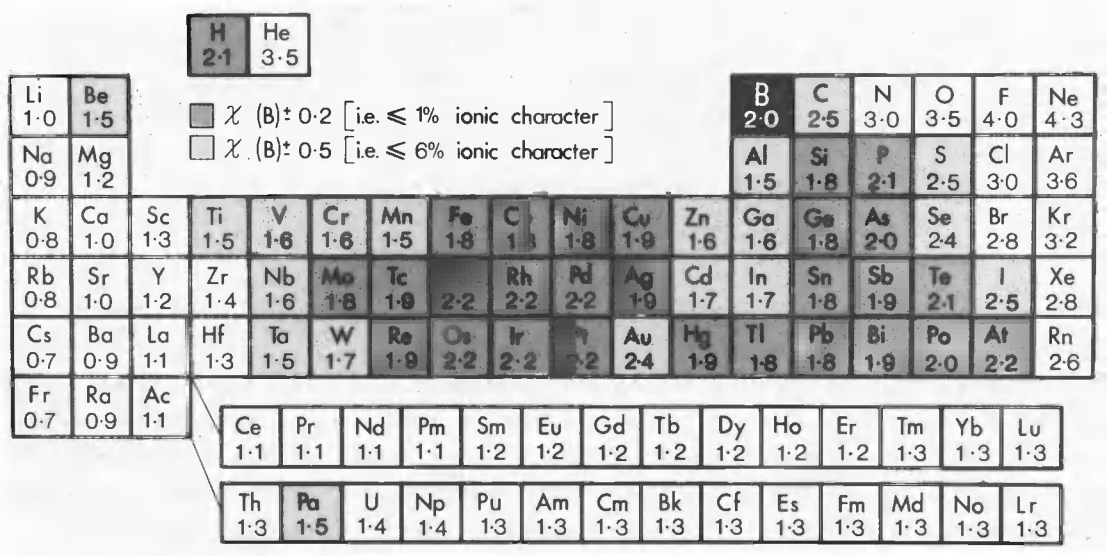


Fig. 1. Electronegativities of the elements: the dark shading indicates those elements whose electronegativities are within ±0.2 of that of boron, whilst the lighter shading covers elements within ±0.5 of an electronegativity unit from boron.

the lanthanoids, and actinoids. The size of the metal does not seem to be important. Nor does the formal oxidation state of the metal, which can be varied to produce just the appropriate number of electrons required by the geometrical series of the cluster formed, i.e. *closo-*, *nido-*, or *arachno-*, etc.

## METALLOBORANE COUNTERPARTS OF KNOWN POLYHEDRAL BORANES

Numerous routes have been devised for the synthesis of metalloborane clusters, and metallo-

borane counterparts of nearly all the parent boranes are known. Sometimes the syntheses are highly selective high-yield routes whilst in other cases a variety of metalloborane compounds may be obtained each in modest or low yield. For example, co-thermolysis of *nido*-$B_5H_9$ with $Fe(CO)_5$ under carefully controlled conditions yields the reactive orange liquid *nido*-$[Fe(\eta^4\text{-}B_4H_8)(CO)_3]$ in which the apical {BH} group of the square-pyramidal $B_5H_9$ has been replaced by an $\{Fe(CO)_3\}$ group, i.e. $[(CO)_3(1\text{-}Fe^{II}B_4H_8)]$ (ref. 4). In both compounds the apical group can be thought of as supplying 2 electrons and 3 orbitals to the cluster bonding. Similarly, *arachno*-$B_5H_{11}$ is apex-subrogated in *arachno*-$[Ir(\eta^4\text{-}B_4H_9)(CO)(PMe_3)_2]$. The compound can be isolated in low yield as a pale yellow, air-stable, diamagnetic solid; it is one of several products from the reaction of *nido*-$B_9H_{12}^-$ with *trans*-$[Ir(CO)Cl(PMe_3)_2]$ (ref. 5) but a much higher yield (~60%) can be obtained by the more direct method of deprotonating *arachno*-$B_4H_{10}$ to give *arachno*-$B_4H_9^-$ and reacting this with an iridium(I) complex such as $[Ir(CO)Cl(PMe_2Ph)_2]$ (ref. 6). It will be noted that the *arachno*-iridapentaboranes $[L_3(1\text{-}Ir^{III}B_4H_9)]$ have two more electrons available for cluster bonding than does the *nido*-ferrapentaborane $[L_3(1\text{-}Fe^{II}B_4H_8)]$, consistent with the expectations of Wade's rules (Table 1).

Metal subrogated derivatives of the hexaboranes are also now well established. For example, replacement of the halide in *trans*-$[Ir(CO)Cl(PPh_3)_2]$ by *nido*-$B_5H_8$ followed by oxidative insertion of the iridium into the base of the cluster affords the pale yellow iridahexaborane *nido*-$[(CO)(PPh_3)_2(2\text{-}IrB_5H_8)]$ (ref. 7); this is closely related structurally to *nido*-$B_6H_{10}$, the formal $\{Ir^{III}(CO)(PPh_3)_2\}$ moiety replacing a basal $\{BH_\mu H_t\}$ unit with which it is "isoelectronic". Likewise, though after a considerably more complex series of reactions, a di-iridahexaborane analogue of *closo*-$B_6H_6^{2-}$ can be prepared by degrading *closo*-$B_{10}H_{10}^{2-}$ in the presence of $[Ir(CO)Cl(PPh_3)_2]$ and methanol (ref. 8); the structure comprises a *cis*-dimetalla 6-atom cluster $\{1,2\text{-}Ir_2B_4\}$ and also features a novel bis(orthocycloboronation) of two of the *P*-phenyl groups on the phosphine ligands associated with one of the iridium atoms, viz. $[1\text{-}\{(CO)_2(PPh_3)\}\text{-}2\text{-}\{(CO)(Ph_2PC_6H_4)_2\}(1,2\text{-}Ir_2B_4H_2)]$.

Metalla derivatives of *closo*-$B_{10}H_{10}^{2-}$, *nido*-$B_{10}H_{14}$, and *arachno*-$B_{10}H_{14}^{2-}$ have been known for some years (ref. 2). Recent examples include:

(a) the bright red *closo*-nickelladecaborane cluster $[(PMe_2Ph)_2(1\text{-}NiB_9H_7Cl_2\text{-}2,4)]$ (Fig. 2a) in which the $B_9$ moiety is $\eta^4$-bonded to the capping $\{Ni^{IV}L_2\}$ group (ref. 9); as the metal centre formally replaces a $BH_t^{2-}$ unit which contributes 4 electrons to the cluster, it can be considered to be $Ni^{IV}$;

(b) the yellow *nido*-iridadecaborane $[H(PPh_3)_2(6\text{-}IrB_9H_{13}]$ (Fig. 2b) and several closely related iridium and rhodium analogues (ref. 10); and

(c) the novel *arachno*-diplatinadecaborane $[(PMe_2Ph)_4(6,9\text{-}Pt_2B_8H_{10}(]$ (Fig. 2c) (ref. 11); the compound is a colourless, very stable, bis-platinum(IV) derivative which can be obtained in good yield by a straight-forward 3-step synthesis from *arachno*-$B_9H_{14}^-$ as follows:

$$2B_9H_{14}^- + \textit{cis}\text{-}[PtCl_2L_2] \xrightarrow[\text{room temp.}]{CH_2Cl_2/12h} [L_2PtB_8H_{12}] \text{ (85\% yield)} \quad (1)$$

$$[L_2PtB_8H_{12}] \xrightarrow[4h,\ \text{room temp.}]{2KH/thf/CH_2Cl_2} [L_2PtB_8H_{10}]^{2-} \text{ (not isolated)} \quad (2)$$

$$[L_2PtB_8H_{10}]^{2-} + \textit{cis}\text{-}[PtCl_2L_2] \xrightarrow[\text{room temp.}]{CH_2Cl_2/12h} [\{L_2Pt\}_2B_8H_{10}] \text{ (55\% yield)} \quad (3)$$

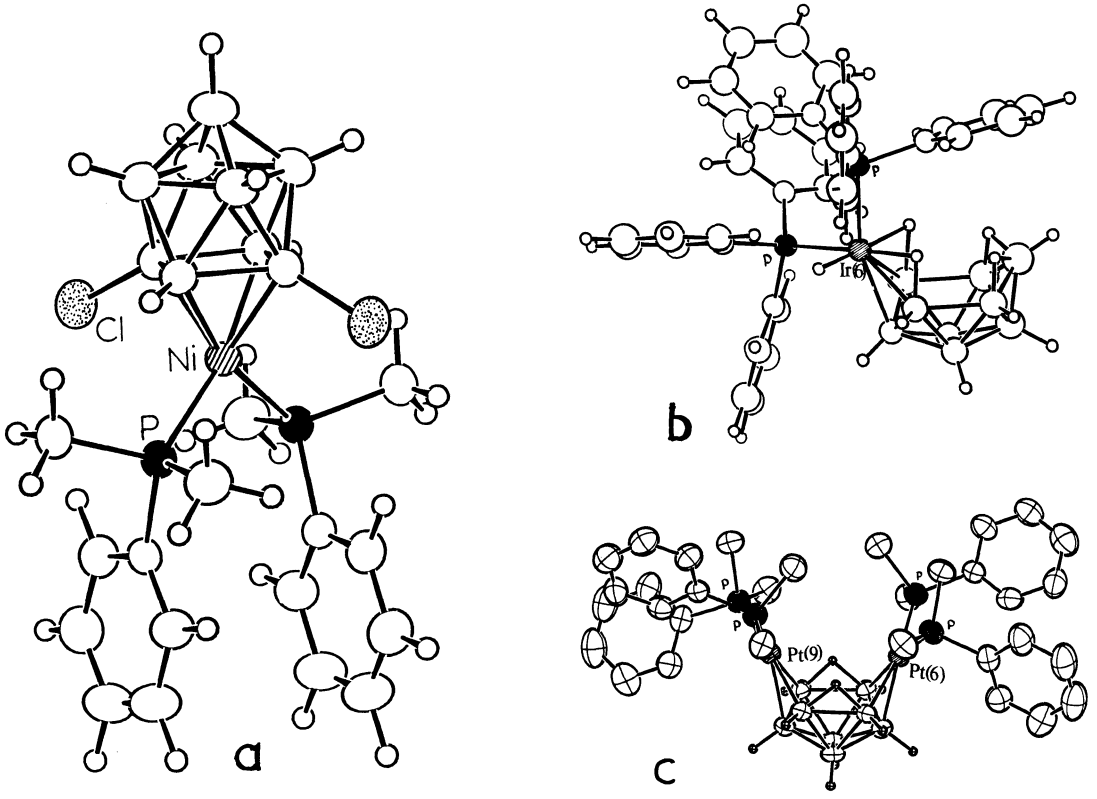


Fig. 2. (a) *closo*-[$(PMe_2Ph)_2(1\text{-}NiB_9H_7Cl_2\text{-}2,4)$], an analogue of *closo*-$B_{10}H_{10}^{2-}$ showing the bicapped square antiprismatic arrangement of the $\{NiB_9\}$ cluster; (b) *nido*-[$H(PPh_3)_2(6\text{-}IrB_9H_{13})$] showing the close similarity to *nido*-$B_{10}H_{14}$; and (c) *arachno*-[$(PMe_2Ph)_4(6,9\text{-}Pt_2B_8H_{10})$] showing the subrogation of the 6- and 9-$\{BH_2^-\}$ units in *arachno*-$B_{10}H_{14}^{2-}$ by $\{Pt^{IV}(PMe_2Ph)_2\}$ groups.

The preceding examples of metalloborane counterparts of known polyhedral boranes is by no means exhaustive and, in addition to metalla- and dimetalla-derivatives of $B_5$, $B_6$, and $B_{10}$ clusters, metalloboranes having any number of vertices from 2 to 12 are known (ref. 2). Whilst this work has undoubtedly been important in devising a variety of routes to metalloboranes and in establishing the range of metals that can be so incorporated, it also raises the intriguing possibility that metal-boron clusters can be synthesized with polyhedral geometries not yet found among the parent borane species themselves. This aspect of the work is discussed in the next section.

## NOVEL POLYHEDRAL CLUSTER GEOMETRIES

If, instead of using *arachno*-$B_9H_{14}^-$ for reaction (1) above, the neutral isoelectronic monoligand derivative 4-$Me_2S$-7-MeO-*arachno*-$B_9H_{12}$ is used, then a 50% yield of the expected *arachno*-platinanonaborane [$(PMe_2Ph)_2(PtB_8H_{11}OMe)$] is obtained, together with a small amount (∿8%) of the known 4-atom cluster [$(PMe_2Ph)_2(PtB_3H_7)$] (ref. 12). In addition, however, two further crystalline, air-stable diplatina-clusters were isolated having structures unparalleled in the chemistry of the parent boranes, viz. [$(PMe_2Ph)_2(Pt_2B_8H_{14})$] (∿3% yield) and [$(PMe_2Ph)_2(Pt_2B_{12}H_{18})$] (∿35% yield). As shown in Figs. 3 and 4, both feature a linear P-Pt-Pt-P unit shared between two borane subclusters. X-ray diffraction analysis established the non-hydrogen atom positions of the *conjuncto*-diplatinadecaborane as in Fig. 3 and

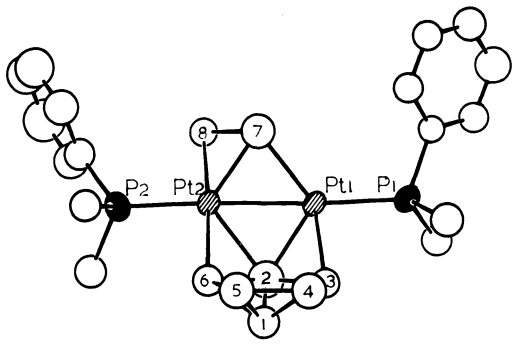


Fig. 3. The cluster geometry of *conjuncto*-[$(PMe_2Ph)_2(Pt_2B_8H_{14})$]. The distance from Pt(1) to Pt(2) is 262.1 pm and to P(1), B(2), B(3) and B(7) are 229, 218, 217, and 222 pm. Distances from Pt(2) to P(2), B(2), B(6), B(7), and B(8) are 229, 218, 228, 216 and 224 pm respectively. The four atoms Pt(1)Pt(2)B(2)B(7) are essentially coplanar (dihedral angle 0.9°) and the central P-Pt-Pt-P group is essentially linear (angles 174.8° and 178.3°).

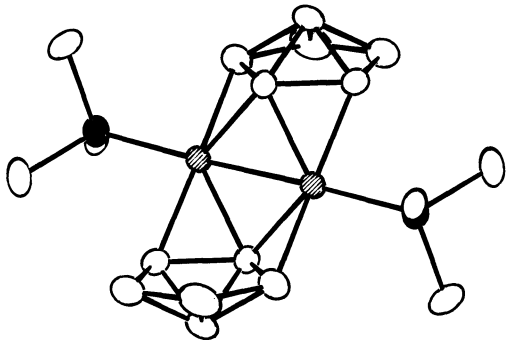

Fig. 4. The cluster geometry of *conjuncto*-[$(PMe_2Ph)_2(Pt_2B_{12}H_{18})$] emphasizing the close relationship to the smaller 10-atom *conjuncto*-cluster in Fig. 3. The Pt-Pt distance is 264.4 pm and distances from the Pt atoms to the 6 attached B atoms are in the range 218-223 pm and to the P atoms 230 pm. The angles Pt-Pt-P=175.5°, and the two *P*-phenyl groups are directly above and below the plane of the paper (i.e. a different ligand orientation to those in Fig. 3).

detailed n.m.r. studies further established the number and disposition of the H atoms on the borane subclusters as $\{B_2H_5\}$ and $\{B_6H_9\}$ respectively. The structure of the 10-vertex cluster is thus entirely different from the *arachno*-diplatinadecaborane cluster found in the precisely isoelectronic compound [$(PMe_2Ph)_4(Pt_2B_8H_{10})$] already described in Fig. 2c. The detailed reaction paths by which the Pt-Pt bond is formed and the initial $B_9$ cluster is degraded to $B_6$ and $B_2$ have not yet been elucidated.

The related *conjuncto*-diplatinatetradecaborane cluster [$(PMe_2Ph)_2(Pt_2B_{12}H_{18})$] (Fig. 4) is a particularly stable species and even survives being heated in air to 200°C. It was first obtained as a biproduct of the reaction of *nido*-decaboranyl oxide, 6,6'-$(B_{10}H_{13})_2O$ with *cis*-$[PtCl_2(PMe_2Ph)_2]$ in neutral dipolar solvents such as $CH_2Cl_2/Et_2O$ at room temperature

(ref. 13), but can be made in better yield (∿15%) using *arachno*-$B_9H_{14}^-$ as the source of the borane groups (ref. 11). Again the detailed course of the reactions remains obscure. One notable feature of the structure of the compound is the *transoid* centrosymmetric disposition of the two $\{\eta^3\text{-}B_6H_9\}$ subclusters; in this it differs from the only known isomer of $B_{14}H_{20}$, which features a *cisoid* disposition of the two $\{B_6H_9\}$ moieties across the central linear H-B-B-H groups (ref. 14). This encourages the thought that the centrosymmetric isomer of $B_{14}H_{20}$ might also be stable and preparable.

A further structural parameter that can be varied is the site of the vertex that is notionally removed when converting a *closo*-cluster into a *nido*-cluster. In the parent boranes this is usually the site of highest connectivity so that, with *nido*-$B_{10}H_{14}$ for example, it is the unique 6-connected vertex of $B_{11}H_{11}^{2-}$ which is removed to give the typical nest-like structure illustrated in Fig 2b for *nido*-iridadecaborane. However, several alternatives can be envisaged and one such is the *iso-nido*-structure obtained as a minor product of the reaction of *arachno*-$B_9H_{14}^-$ with $[IrCl(PPh_3)_3]$ at room temperature: the major product (>85% yield) is again the yellow complex shown in Fig. 2b but trace quantities of the pale-violet *iso-nido*-iridadecaborane $[(PPh_3)_2(7\text{-}IrB_9H_{10}.PPh_3)]$ are also obtained (ref. 15). As shown in Fig. 5, the $\{Ir(PPh_3)_2\}$ group now occupies the high-connectivity apical site

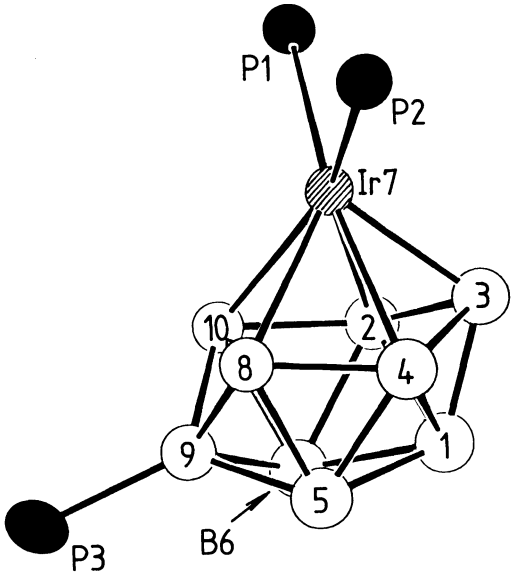


Fig. 5. The molecular structure of *iso-nido*-$[PPh_3)_2(7\text{-}IrB_9H_{10}.PPh_3)]$ (see text). Distances from Ir(7) to B(2,3,4,8,10) are 237, 211, 232, 233, and 233 pm respectively, and the distance B(8)-B(10) across the "open" face is ∿211 pm, suggesting some residual interactions (as represented by the open connector in the diagram).

whilst the vertex above the Ir(7)B(8)B(9)B(10) face (i.e. the site equivalent to B(3) on the right hand side of the structure) is missing. There are terminal H atoms on each boron except B(9) (which carries a pendant $PPh_3$ ligand) and the two remaining H atoms are associated with the open face Ir(7)B(8)B(9)B(10): they are inequivalent in solution at low temperature but undergo mutual exchange with $\Delta G^{\ddagger}$ ∿45 kJ $mol^{-1}$ at -10°C. In fact, as indicated in the caption to Fig. 5, there is a fairly close approach across the open face between B(8) and B(10) and the cluster is in some sense intermediate between a *nido*- and a *closo*-geometry, with Ir-$H_\mu$-B bridge hydrogen atoms interconverting with Ir-$H_t$.

An even more extensive modification has been achieved in the *closo*-decaborane series. Here the normal structure is the bicapped square antiprism as exemplified by *closo*-$B_{10}H_{10}^{2-}$ itself and its many apex- and equatorial-subrogated metal derivatives such as the nickella-complex in Fig. 2a. However, it has recently been shown (ref. 16) that mild thermolysis of $[H(PPh_3)_2(IrB_9H_{13})]$ (Fig. 2b) at 85° results in the smooth elimination of $3H_2$ and the quantitative production of the orange-yellow *iso-closo*-$[H(PPh_3)(PPh_2\overline{C_6H_4})(1\text{-}Ir\overline{B_9H_8})]$. This has the unprecedented structure shown in Fig. 6. Other high-yield routes from *nido*-$B_9H_{12}^-$

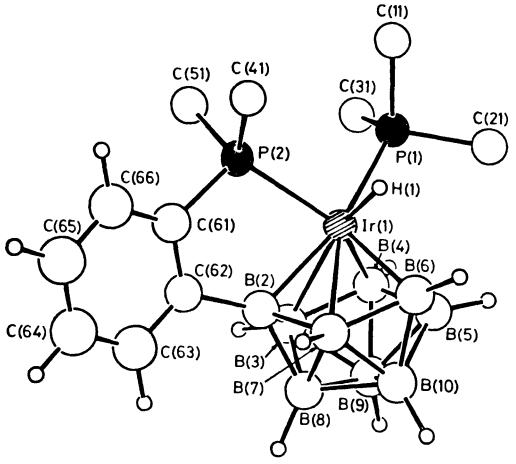


Fig. 6. The molecular structure of *iso-closo*-$[H(PPh_3)(PPh_2\overline{C_6H_4})(1\text{-}Ir\overline{B_9H_8})]$ showing the idealized $C_{3v}$ symmetry of the cluster i.e. Ir(1)B(2,4,6)-B(3,5,7)B(8,9,10). The *P*-phenyl groups have been omitted for clarity (except for their *ipso* C atoms). Distances from Ir(1) to B(2,4,6) are 216, 219, and 215 pm and to B(3,5,7) are 246, 239, 238 pm respectively. The cross-cluster distances B(2,4), B(4,6), and B(6,2) are all clearly non-bonding at 295-301 pm. All H atoms were located and Ir-H is ∿157 pm.

are also available. The cluster is seen to have local 3-fold rather than 4-fold symmetry and the geometry can be represented as $IrB_3B_3B_3$. A further interesting aspect of the structure is the *ortho*-cycloboronation at B(2), as previously also noted in *closo*-$[(CO)_3(PPh_3)(PPh_2\overline{C_6H_4}_2)(Ir_2\overline{B_4H_2})]$ above, and this is now recognised as a significant feature of several cluster reorganization reactions (e.g. refs. 8, 16, 17, 18). A formal electron count requires 22 electrons (2n+2) for the *closo* 10-vertex cluster bonding; of these, 18 are supplied by the 9 B atoms, leaving 4 to be contributed by the Ir atom. This, together with the Ir-$H_t$ bond, indicates that the compound can be regarded as an $Ir^V$ complex in which the high oxidation state is stabilized by coordination to the polyhedral borane ligand. Other examples of $Ir^V$ borane complexes are in ref. 17, and in ref. 19 (below).

The normal 9-vertex *closo*-polyhedron is a tricapped trigonal prism (ref. 3) and this has always been found to be the preferred geometry. However, other closed triangulated polyhedra can be imagined and one of these has recently been synthesized by dehydrogenation of the related *arachno*- and *nido*-structures (ref. 19), e.g.

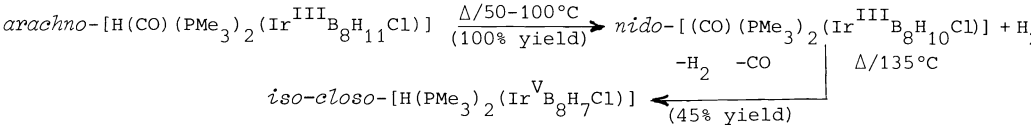

The poppy-red product, *iso-closo*-[H($PMe_3$)$_2$($IrB_8H_7Cl$)], has the previously unobserved cluster geometry shown in Fig. 7: it has idealized $C_{2v}$ symmetry with an $\eta^6$ borane-to-metal coordination mode. The six boron atoms B(2,3,4,5,6,7) adopt an inverted boat configuration with respect to the apical Ir atom, and the six Ir-B distances are all in the range 217.7-219.4 pm. There is no significant bonding across the cluster between B(2)···B(4) (307 pm) or between B(5)···B(7) (304 pm) as would have been observed in the tricapped trigonal prismatic arrangement.

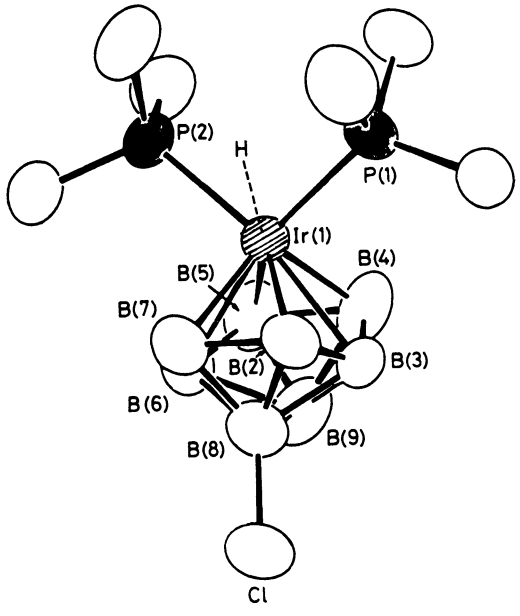


Fig. 7. The molecular structure of *iso-closo*-[H($PMe_3$)$_2$($IrB_8H_7Cl$)] (see text).

MACROPOLYHEDRAL BORANES

So far we have been considering metalloboranes which have direct structural counterparts amongst the parent boranes, or which have novel cluster geometries not so far observed amongst the boranes and borane anions or their simple derivatives such as the carbaboranes and ligand-adducts. A further extension would be to construct larger conjuncto clusters having a number of vertices so far unencountered amongst the parent borane species. There is, for example, no known 17-vertex cluster but one can be synthesized by the mild thermolysis of the known 9-vertex compound *arachno*-[($PMe_2Ph$)$_2$($PtB_8H_{12}$)] which can itself be readily prepared in high yield according to reaction (1) above.

Thermolysis in boiling toluene at ∿110°C for 1.5 h gives several products among which is the air-stable flame-red *conjuncto*-[($PMe_2Ph$)(7-$PtB_{16}H_{18}$.$PMe_2Ph$)] which was obtained in ∿2% yield (ref. 20). The structure is shown in Fig. 8a; it comprises an edge-fused *conjuncto*-metalloborane consisting of a *nido*-{$PtB_7$} unit joined to a *nido*-{$PtB_{10}$} unit via a common Pt-B edge. The compound can be regarded as a complex between the macropolyhedral borane ligand $\eta^6$-{$B_{16}H_{18}$($PMe_2Ph$)}$^{4-}$ ligand and a {Pt($PMe_2Ph$)}$^{4+}$ metal centre as indicated in Fig. 8b. The ligand is thus a phosphine-substituted 16-vertex unit derived from the as yet unknown *conjuncto*-hexadecaborane, $B_{16}H_{24}$, and the complex has considerable significance in the general field of polyhedral borane synthesis.

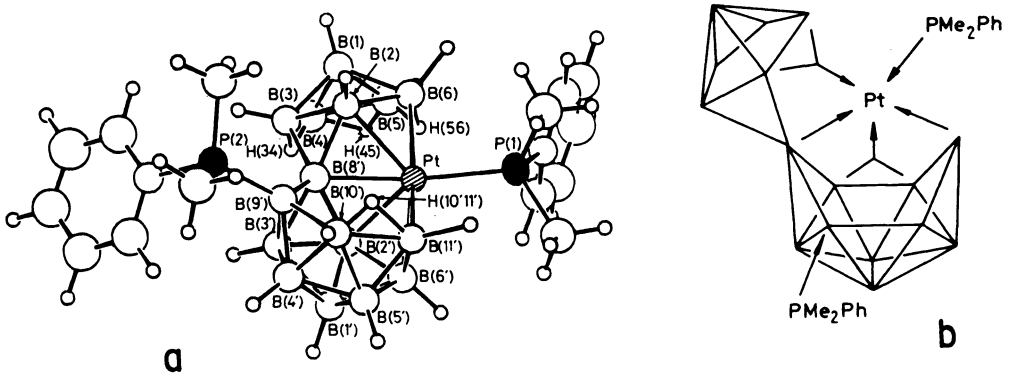


Fig. 8(a). The molecular structure of the 17-vertex *conjuncto*-platinaborane [$(PMe_2Ph(7\text{-}PtB_{16}H_{18}.PMe_2Ph)]$. The distances from Pt(7) sequentially to B(6,2,8',2',6',11') are 227, 224, 223, 224, 225, and 229 pm. (b) An outline diagram of the macropolyhedral borane ligand geometry and its interaction with the Pt centre.

Finally, there is time to allude briefly to the elegant structural chemistry that has been unravelled in characterizing the numerous products which are formed when the *syn*- and *anti*-isomers of *conjuncto*-$B_{18}H_{22}$ are deprotonated and the resulting anions reacted with *cis*-$[PtCl_2(PMe_2Ph)_2]$ (ref. 21). The parent borane isomers derive from the two possible ways of edge-fusing two *nido*-$B_{10}$ clusters, the *anti*-isomer being centrosymmetric. Figs. 9a and 9b show the observed structures of the expected products $[(PMe_2Ph)_2(Pt\text{-}\eta^4\text{-}syn\text{-}B_{18}H_{20})]$ and $[(PMe_2Ph)_2(Pt\text{-}\eta^4\text{-}anti\text{-}B_{18}H_{20})]$. In addition to these yellow air-stable complexes, several

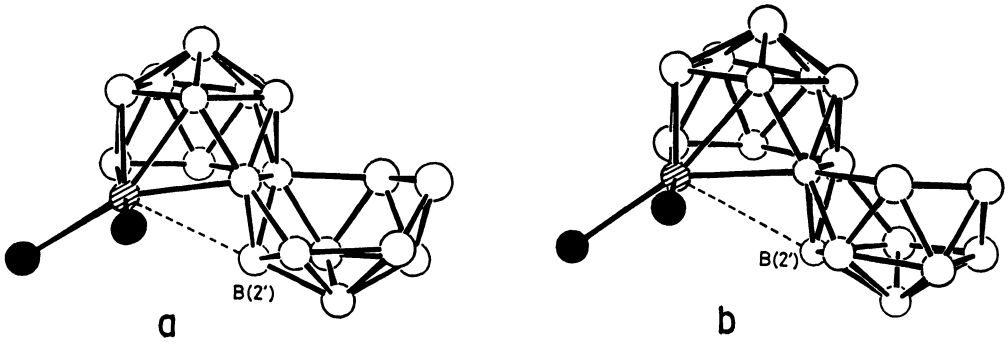


Fig. 9(a). The molecular structure of the isomeric $[(PMe_2Ph)_2(Pt\text{-}\eta^4\text{-}syn\text{-}B_{18}H_{20})]$; Pt-B distances within the $\eta^4$-bonding mode are 231, 225, 224, and 235 pm respectively. (b) the moelcular structure of the isomeric $[(PMe_2Ph)_2(Pt\text{-}\eta^4\text{-}anti\text{-}B_{18}H_{20})]$; in this complex the four Pt-B distances are 236, 227, 224, and 234 pm respectively.

other products are obtained including the unprecedented Pt-bridged $\eta^1,\eta^2$-isomer shown in Fig. 10a - the relation to the $\eta^4$-*anti* isomer in Fig. 9b is clear, the Pt atom now bridging the two rear boron atoms B(9)B(10) and the B(2') apex of the second cluster. Thermolysis of this Pt-bridged isomer results in an astonishing cluster rearrangement in which the $\{PtL_2\}$ group transfers to the second cluster and new connections are forged between B(9), B(10), and B(2') with concurrent elimination of $H_2$. The resulting compound $[(PMe_2Ph)_2(Pt\text{-}\eta^4\text{-}anti\text{-}B_{18}H_{18})]$, has a shared triangular face between the two clusters as shown in Fig. 10b. The same feature is observed in a unique, green, diplatina product isolated from the original reaction mixture,

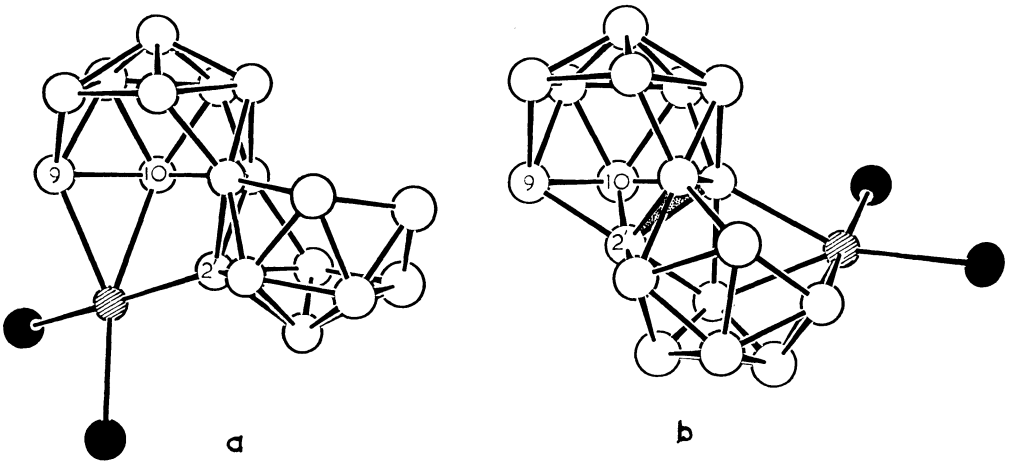


Fig. 10(a). The molecular structure of the isomeric $[(PMe_2Ph)_2(\mu\text{-Pt-}\eta^1,\eta^2\text{-}anti\text{-}B_{18}H_{20})]$; the interatomic distance from Pt to B(2') is 212 pm ($\eta^1$) and the ($\eta^2$-distances to B(9) and B(10) are 229 and 232 pm. (b) The molecular structure of the thermolysis product $[(PMe_2Ph)_2(Pt\text{-}\eta^4\text{-}anti\text{-}B_{18}H_{20})]$ showing the new confacial triangular feature (shaded) between the two clusters. Pt-B distances are 234, 227, 220, and 224 pm.

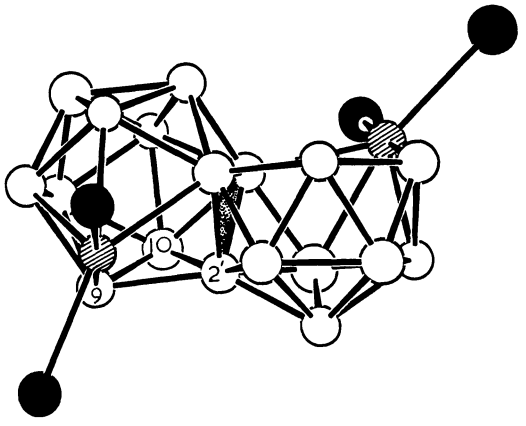


Fig. 11. The molecular structure of the green diplatina product $[(PMe_2Ph)_4\{Pt_2\text{-}\eta^4,(\eta^4+\eta^2)\text{-}anti\text{-}B_{18}H_{16}\}]$ showing the confacial fusion of the two clusters across the shaded triangle.

viz. $[(PMe_2Ph)_4\{Pt_2\text{-}\eta^4,(\eta^4+\eta^2)\text{-}anti\text{-}B_{18}H_{16}\}]$ (Fig. 11). The 7-fold connectivity of the three confacial B atoms is noteworthy. Further details are in ref. 21.

## CONCLUSIONS

The field of metalloborane complexes has developed into one of the major areas of cluster chemistry. Not only can metals be incorporated as vertices in the known boron hydride structures, but new cluster geometries can be made which have, as yet, no counterparts among the boranes themselves. The flexibility introduced by use of metal vertices within the polyhedral clusters enables points of low or high connectivity to be incorporated, and the potential variability of the metal oxidation state introduces a further flexibility. As in other areas of coordination chemistry and organometallic chemistry, fine tuning can be

effected by varying the attached ligands, and this can be subtly exploited in the synthesis of new and previously unsuspected cluster types. The gross aspects of structure and bonding in these polyhedral metalloborane clusters have been established but many important points of detail await clarification. The elucidation of synthetic pathways and the detailed mechanisms of cluster expansion, degradation, and rearrangement also provide many exciting challenges for future research.

ACKNOWLEDGEMENTS

The experimental skill, chemical insight, and tremendous enthusiasm of members of the Leeds borane group are abundantly clear from the work described in the individual publications cited below - their imagination and creativeness has made this lecture possible.

REFERENCES

1. N.N. Greenwood (convenor) Microsymposium 1. Boranes as Ligands, *Proc. 19th Int. Conf. Coord. Chem.*, Vol. 1, 69-88, Prague, Sept. 4-8, 1978.
2. N.N. Greenwood and J.D. Kennedy, Chap. 2 in R.N. Grimes *Metal Interactions with Boron Clusters*, Plenum Press, New York, 1982.
3. K. Wade, *Adv. Inorg. Chem. Radiochem.* 18, 1-66 (1976).
4. N.N. Greenwood, C.G. Savory, R.N. Grimes, L.G. Sneddon, A. Davison, and S.S. Wreford, *J.C.S. Chem. Comm.*, 718 (1974).
5. J. Bould, N.N. Greenwood, and J.D. Kennedy, *J.C.S. Dalton*, 481-483 (1982).
6. S.K. Boocock, M.J. Toft, and S.G. Shore, Abstract INOR 149, *182nd ACS National Meeting*, New York, 23-28 August, 1981.
7. N.N. Greenwood, J.D. Kennedy, W.S. McDonald, D. Reed, and J. Staves, *J.C.S. Dalton*, 117-123 (1979).
8. J.E. Crook, N.N. Greenwood, J.D. Kennedy, and W.S. McDonald, *J.C.S. Chem. Comm.*, 383-384, (1982).
9. M.J. Hails, PhD Thesis, University of Leeds, 1981.
10. S.K. Boocock, J. Bould, N.N. Greenwood, J.D. Kennedy, and W.S. McDonald, *J.C.S.Dalton*, 713-719 (1982).
11. S.K. Boocock, N.N. Greenwood, M.J. Hails, J.D. Kennedy, and W.S. McDonald, *J.C.S. Dalton*, 1415-1429 (1981).
12. R. Ahmad, J.E. Crook, N.N. Greenwood, J.D. Kennedy, and W.S. McDonald, *J.C.S.Chem. Comm.*, in press.
13. N.N. Greenwood, M.J. Hails, J.D. Kennedy, and W.S. McDonald, *J.C.S. Chem. Comm.*, 37-38, (1980).
14. J.C. Huffmann, D.C. Moody, and R. Schaeffer, *J. Am. Chem. Soc.*, 97, 1621-1622, (1975).
15. J. Bould, N.N. Greenwood, J.D. Kennedy, and W.S. McDonald, unpublished work.
16. J. Bould, N.N. Greenwood, J.D. Kennedy, and W.S. McDonald, *J.C.S. Chem. Comm.*, 465-467, (1982).
17. J.E. Crook, N.N. Greenwood, J.D. Kennedy, and W.S. McDonald, *J.C.S. Chem. Comm.*, 933-934 (1981).
18. N.N. Greenwood in M.H. Chisholm (ed.) *Inorganic Chemistry Toward the 21st Century*, Bloomington, Indiana, May 16-19, 1982, ACS Symposium Series, in press.
19. J. Bould, J.E. Crook, N.N. Greenwood, J.D. Kennedy, and W.S. McDonald, *J.C.S. Chem. Comm.*, 346-348 (1982).
20. M.A. Beckett, J.E. Crook, N.N. Greenwood, J.D. Kennedy, and W.S. McDonald, *J.C.S. Chem. Comm.*, 552-553, (1982).
21. Y.M. Cheek, N.N. Greenwood, J.D. Kennedy, and W.S. McDonald, *J.C.S. Chem. Comm.*, *80-81*, (1982).